



A Search for Charged Massive Stable Particles at DØ

The DØ Collaboration
URL <http://www-d0.fnal.gov>
(Dated: March 3, 2005)

A search for charged massive stable particles has been performed with the DØ detector at the Fermilab Tevatron. The signature is two particles reconstructed as muons, but with speed and invariant mass inconsistent with beam-produced muons. No excess of events is observed and limits are set on the production cross-section for pair-produced stable stau sleptons based on 390 pb^{-1} of data. Limits vary from 0.06 pb to 0.62 pb, depending on the stau mass, and are the strictest Tevatron limits to date. Mass limits are also set for stable charginos. The limits are 140 GeV for a higgsino-like chargino and 174 GeV for a gaugino-like chargino. These are currently the best limits to date for stable charginos.

Preliminary Results for Winter 2005 Conferences

I. INTRODUCTION

This analysis is a search for new particles that are electrically charged and have a lifetime long enough to escape the entire detector before decaying. Although cosmological considerations put strict limits on new particles that are absolutely stable, these restrictions do not apply to particles that live long enough to decay outside the detector [1, 2]. The term *stable* in this note will refer to particles that live long enough to escape the detector before decaying.

The detector signature of a stable charged particle is dramatic. These particles will lose energy principally by ionization and will be able to traverse the entire detector, registering in the muon detectors. However, since these particles will be fairly massive (more than about 100 GeV), they will be traveling substantially slower than the speed of light. Beam-produced muons, on the other hand, must be traveling at the speed of light in order to penetrate to the outermost layers of the detector. Additionally, since the charged massive stable particles (CMSP's) are moving relatively slowly, the Bethe-Bloch formula predicts that their ionization energy loss will be greater than that for a speed-of-light muon. A meaningful limit can be set using the muon system timing information alone, without using the additional discrimination from energy loss, so this analysis only uses timing information in the muon system.

There are several possible models which could result in a CMSP. For example, supersymmetric models can predict either the lightest chargino or the lightest stau slepton to have a lifetime long enough to decay outside the detector.

One theoretical model explored in this note is Gauge-Mediated Supersymmetry Breaking (GMSB) [3, 4]. All GMSB models contain a very light gravitino/goldstino as the lightest supersymmetric particle (LSP) and hence the phenomenology is driven by the next-to-lightest supersymmetric particle (NLSP). The NLSP can be either the lightest neutralino or the lightest scalar tau lepton (stau), depending on the choice of model parameters [26]. It is possible for a stau NLSP in these models to be long-lived [5]. It has been suggested that if the gravitino/goldstino is the LSP, then the NLSP should be long lived [6, 7].

The GMSB model used in this analysis is a model with a stau NLSP. It is referred to as ‘‘Model Line D’’ from the Snowmass 2001 Direct Investigations of Supersymmetry Subgroup [8]. The parameters of this model are shown in Table I. If the stau decays to the gravitino/goldstino are sufficiently suppressed (through a large value of the C_{grav} parameter), then the stau lives long enough to escape the detector. If the stau NLSP is stable, then all heavier SUSY particles will first decay to a stau before decaying to the gravitino/goldstino LSP. However, the signature of these cascade decays in the detector is quite model dependent and can be difficult to simulate accurately. In this analysis, only the pair-production of the lightest staus is considered. This means that each signal event will contain exactly two stable staus. However, this analysis will also have some sensitivity to events containing CMSP's produced in cascade decays. The background estimates are unchanged for such topologies but the (highly model-dependent) signal acceptance will be different than that quoted for this analysis.

TABLE I: GMSB Model Parameters

Parameter	Description	Value
Λ_m	Scale of SUSY breaking	19 to 100 TeV
M_m	Messenger mass scale	$2\Lambda_m$
N_5	Number of messenger fields	3
$\tan\beta$	Ratio of Higgs VEVs	15
$\text{sgn}\mu$	Sign of Higgsino mass term	+1
C_{grav}	Factor multiplying effective mass of gravitino	1

Another model explored in this note includes the stable lightest chargino which can have a lifetime long enough to escape the detector if the mass difference between the lightest chargino and the lightest neutralino is less than about 150 MeV [9, 10]. This situation can occur in Anomaly-Mediated Supersymmetry Breaking (AMSB) or in models that do not have gaugino mass unification. There are two general cases. One is where the chargino is mostly higgsino and the other is when the chargino is mostly gaugino. These two cases are treated separately in the analysis. The parameters used to generate charginos in the two cases are shown in Table II. As in the stau analysis, only the pair production of charginos was considered.

TABLE II: SUSY parameters used in chargino analysis

Model	μ (GeV)	M_1 (GeV)	M_2 (GeV)	M_3 (GeV)	$\tan\beta$	Squark Mass (GeV)
higgsino-like chargino	varied from 60 to 300	100,000	100,000	500	15	800
gaugino-like chargino	10,000	$3M_2$	varied from 60 to 300	500	15	800

Several collider experiments, both at the Tevatron and at LEP, have performed searches for CMSP's. The CDF

experiment has placed cross section limits for a stable slepton based on data from Run I that vary from 1.3 pb (for a mass of 80 GeV) to 0.75 pb (for a mass of 120 GeV) [11]. Searches at the LEP experiments have resulted in mass limits for a stable slepton that vary from 77 GeV to 102 GeV [12–15]. Searches have also been performed for stable charginos. Experiments at LEP have placed mass limits on stable charginos that vary from 87.5 GeV to 102.0 GeV [16–20]. A preliminary combination of all LEP results has excluded stable charginos in the mass range from 45 GeV to 102.5 GeV at the 95% confidence level [21].

II. SIGNAL AND DATA SAMPLE

Pythia 6.202 was used to generate signal events for both the stau and the chargino analysis [22]. Events were generated at mass points of 60, 100, 150, 200, 250, and 300 GeV. A parameterized Monte Carlo simulation (PMCS) was used to simulate the detector response. PMCS includes all detector resolution smearing, trigger, and muon identification efficiencies as measured in $Z \rightarrow \mu\mu$ events. PMCS also simulates the timing of the muon scintillation counters. The muon times are smeared according to resolutions and offsets measured in muons in data.

The data sample consists of all data taken by the DØ detector from April 2002 through August 2004. The trigger requires two muons to be present in the event. There is a finite trigger time gate during which a muon must arrive in order to satisfy the trigger. This effectively limits the sensitivity to particles with a speed greater than approximately half the speed of light. After trigger and data quality requirements, the data sample has an integrated luminosity of 390 pb^{-1} . The preselection cuts require two muons to be reconstructed in the events. Each muon is required to have a transverse momentum greater than 15 GeV, be matched to a track in the central tracker, and have scintillator hits in at least two of the three layers of scintillators in the detector. At least one of the muons in the event must be isolated (in the calorimeter and the central tracker). The two muons in the event are also required to have a difference in ϕ larger than 1.0 radians, where ϕ is the azimuthal angle measured around the beam line. Cosmic ray muon vetos are also performed, as a cosmic ray muon can mimic the signal of an out-of-time muon.

The timing information in the muon system is used to calculate the speed of the two particles in the event. For each particle, the speed and its uncertainty are calculated for each layer of scintillators where hits are present. The uncertainty is calculated from the time resolution of each type of scintillation counter, as measured in data. The speed measurements for each layer containing scintillator hits are then combined to form an average speed. The χ^2 of this average speed (as compared to the individual layer speeds) is then calculated. To ensure that the speed of both particles in the event is well measured, a cut is applied requiring the χ^2 per degree of freedom of the speed measurement for each particle in the event to be less than four. This cut will remove background events that were not beam-produced, such as cosmic ray muons and hadronic particles that escape the calorimeter and register in the muon system, and will also remove events whose scintillator time is in the non-gaussian tail of the timing distribution.

III. ANALYSIS CUTS

As its principal selection criterion, this analysis uses the slow-moving character of heavy stable particles. The speed of the particle, as calculated from the average of all layer speeds, and the uncertainty on the average speed is used to define the *speed significance*, as shown in equation 1.

$$\text{speed significance} = \frac{1 - \text{speed}}{\sigma_{\text{speed}}} \quad (1)$$

The speed significance is a measure of the number of standard deviations away from the speed of light. Since CMSP's will be moving slower than the speed of light, they are expected to have a speed significance that is larger than zero. Particles moving at the speed of light are expected to have a speed significance of zero (within the detector resolution). Figure 1 shows the speed significance for real muons in data, 100 GeV, and 300 GeV staus. The speed significance of muons in data has a slight asymmetry, with a longer tail at positive speed significance. This is because the readout window for the scintillator times is asymmetric, accepting times up to approximately 60 ns after the beam-produced muon signal, but only as early as about 20 ns before beam muon times. Finally, the speed significance of both particles in the event is multiplied to obtain the *significance product*.

A cut is applied to require the speed significance of both particles in the event to be greater than zero. Since the speed significance product will be used in the next cut, this cut removes events with the speed significance of both particles negative, which would result in a positive significance product.

Signal particles have a larger transverse momentum than muons from Z boson decays or Drell-Yan production, as shown in figure 2. Hence, signal events have a larger invariant mass than background muons. The significance

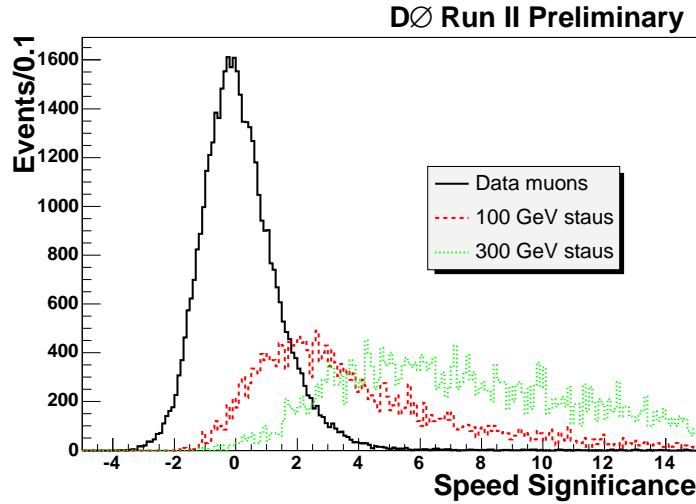


FIG. 1: Speed significance for real muons in data (solid black line), 100 GeV staus (dashed red line), and 300 GeV staus (dotted green line). All particles pass preselection cuts. Histograms are normalized to approximately the same number of events.

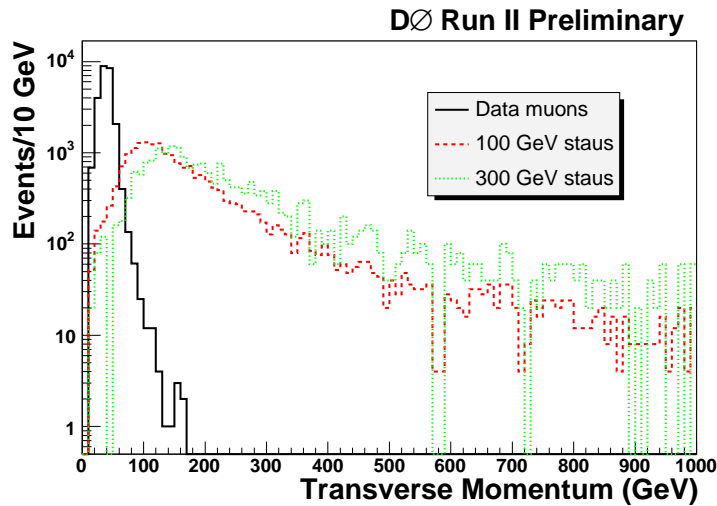


FIG. 2: Transverse momentum for real muons in data (solid black line), 100 GeV staus (dashed red line), and 300 GeV staus (dotted green line). All particles pass preselection cuts. Histograms are normalized to approximately the same number of events.

product and invariant mass of signal events show a positive correlation, while these quantities are uncorrelated for background events. The final cut applied is a hyperbolic cut in the invariant mass-significance product plane. Due to the very small number of stau events expected (based on the cross section), this cut was optimized with respect to the expected 95% confidence level cross section limit (for stable staus) for each of the six mass points. The two-dimensional distribution of invariant mass and significance product for data events and 60 GeV stau signal events, with the optimized cut, are shown in Figure 3.

There are no known physics backgrounds that would appear in the detector as a massive, slow-moving particle, so the background is estimated from data. Since the significance and invariant mass of background events show no significant correlation, the background rejection for each cut is calculated separately, then multiplied together to get the total background rate.

The rejection rate for background events due to the significance cuts was estimated using muons in the Z-peak (invariant mass from 80 to 100 GeV). There are over ten thousand data events in this invariant mass range, while less than one signal event would be expected. In order to estimate the background rejection of the two-dimensional cut in the invariant mass versus significance product plane, two distributions were used. The first was the significance product distribution of data events in the Z peak (80 to 100 GeV). The second was the invariant mass distribution of

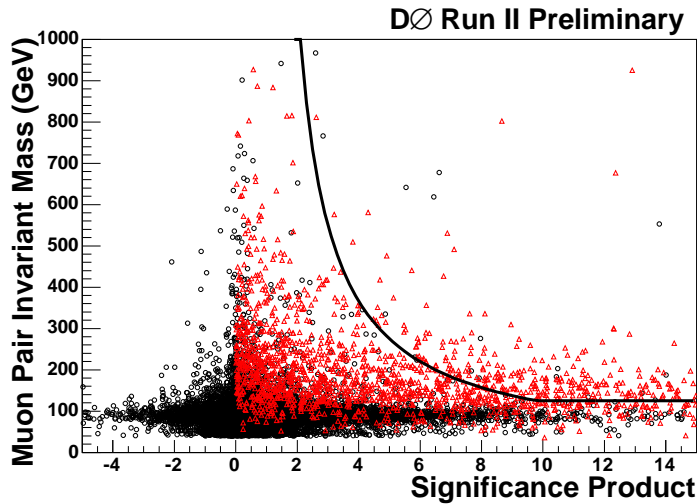


FIG. 3: Invariant mass versus significance product for real muons in data (black circles) and 60 GeV staus (red triangles). All particles pass preselection cuts. Histograms are normalized to approximately the same number of events. The optimized two-dimensional cut is shown as a black line. All events above the line are passed.

TABLE III: Events remaining and signal acceptance after cuts, 100 GeV staus.

Cut	Data Events	Predicted background	Signal Acceptance
Preselection	18,985		0.19
Significance > 0	6410	$6279 \pm 127 \pm 44$	0.17
Invariant mass vs. speed significance cut	0	$0.66 \pm 0.06 \pm 0.02$	0.06

data events where the speed significance of both particles is negative (the signal contamination would be negligible in this region). These two distributions are used to construct the two dimensional probability density function, which is integrated to get the final background rejection of the two-dimensional cut.

IV. RESULTS

The events remaining after the various cuts are shown in Table III for staus with a mass of 100 GeV. Table IV shows the final number of events remaining in the data, the signal acceptance, and the predicted number of background events for all six stau mass points.

The signal acceptance has several sources of systematic uncertainty. The uncertainty on the PMCS simulation of the trigger and muon identification has been estimated at 2%. This value was obtained by varying the relevant efficiencies in PMCS by their estimated uncertainties. Additionally, a systematic uncertainty due to the simulation of the muon timing is estimated by changing the resolutions and offsets used in the simulation. The systematic uncertainty due to the timing is estimated at 1.9%. The efficiency for signal events to pass the χ^2 preselection requirement was estimated from data and has an estimated systematic uncertainty less than 1%. The total systematic uncertainty on the signal acceptance is obtained by adding these three values in quadrature, resulting in a value of 2.7%.

TABLE IV: Analysis results for all six stau mass points.

Stau Mass (GeV)	Data Events	Background Prediction	Signal Acceptance
60	13	13.6 ± 0.7 (stat) ± 0.5 (syst)	0.0381 ± 0.0007 (stat) ± 0.0010 (syst)
100	0	$0.66 \pm 0.06 \pm 0.02$	$0.0559 \pm 0.0009 \pm 0.0015$
150	0	$0.69 \pm 0.05 \pm 0.02$	$0.0968 \pm 0.0014 \pm 0.0026$
200	0	$0.60 \pm 0.04 \pm 0.02$	$0.1180 \pm 0.0016 \pm 0.0032$
250	0	$0.47 \pm 0.03 \pm 0.02$	$0.1222 \pm 0.0017 \pm 0.0033$
300	0	$0.61 \pm 0.05 \pm 0.02$	$0.1226 \pm 0.0017 \pm 0.0033$

TABLE V: Limits and NLO cross section for pair-produced staus.

Stau Mass (GeV)	95% CL limit (pb)	NLO cross section (pb)
60	0.620	0.072
100	0.139	0.012
150	0.081	0.0022
200	0.066	0.00049
250	0.064	0.00012
300	0.064	0.000032

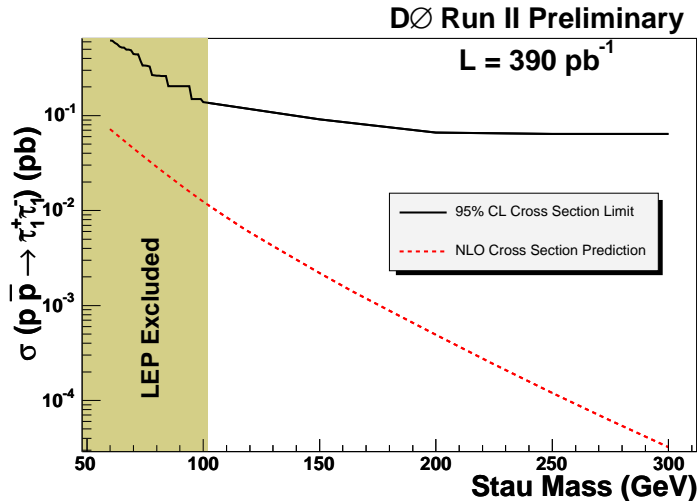


FIG. 4: 95% CL cross-section limit (solid line) and NLO production cross section (dashed line) versus stau mass for pair-produced staus.

Each of the analysis cuts applied can contribute to the systematic uncertainty on the background estimation. The size of these systematic uncertainties is estimated by varying the criteria used to select events for the background efficiency measurement. The total systematic uncertainty on the background estimate has been estimated at 3.6%.

Since the number of observed events is consistent with the expected background, a 95% confidence level limit on the production cross section is set using the CL_s method for each stau mass point [23]. These can be compared to the next-to-leading order cross section calculated with SoftSusy and Prospino 2 [24, 25]. The calculated limits and the NLO cross section for each mass point are shown in Table V and graphically in Figure 4. Although these limits are not yet stringent enough to set a limit on the stau mass, they are the best limits to date from the Tevatron.

The kinematic properties of pair-produced chargino events are similar to pair-produced stau events. This can be seen in Figure 5, which shows the speed distribution for 100 GeV staus overlaid with 100 GeV higgsino-like and chargino-like charginos. Since the distributions are similar, the same cuts are used for the chargino mass points that were used for staus. The signal acceptance for the two chargino models is shown in Table VI.

A 95% confidence level cross section limit on the pair production cross section was set for both chargino models. This is compared to the predicted next-to-leading order cross section. The limits obtained and the NLO cross section are shown for both of the chargino models in Table VII. This is shown graphically in Figure 6 for the higgsino-like

TABLE VI: Signal acceptance for the two chargino models.

Stau Mass (GeV)	Higgsino-like Signal Acceptance	Gaugino-like Signal Acceptance
60	0.0249 ± 0.0006 (stat) ± 0.0007 (syst)	0.0227 ± 0.0005 (stat) ± 0.0006 (syst)
100	$0.0519 \pm 0.0009 \pm 0.0014$	$0.0536 \pm 0.0009 \pm 0.0015$
150	$0.0815 \pm 0.0012 \pm 0.0022$	$0.0805 \pm 0.0012 \pm 0.0022$
200	$0.0921 \pm 0.0013 \pm 0.0025$	$0.0880 \pm 0.0013 \pm 0.0024$
250	$0.0872 \pm 0.0013 \pm 0.0024$	$0.0814 \pm 0.0012 \pm 0.0022$
300	$0.0783 \pm 0.0012 \pm 0.0021$	$0.0733 \pm 0.0011 \pm 0.0020$

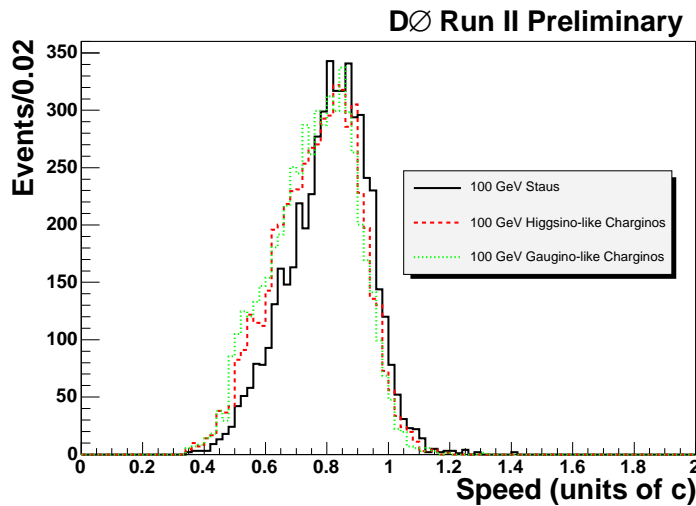


FIG. 5: Speed distribution for staus (solid black line), higgsino-like charginos (dashed red line), and gaugino-like charginos (dotted green line). Both the staus and charginos have a mass of 100 GeV. All particles pass preselection cuts. Histograms are normalized to the same number of events.

TABLE VII: Limits and NLO cross section for pair-produced charginos.

Chargino Mass (GeV)	Higgsino-like 95% CL limit (pb)	Higgsino-like NLO cross section (pb)	Gaugino-like 95% CL limit (pb)	Gaugino-like NLO cross section (pb)
60	0.947	3.11	1.039	13.39
100	0.150	0.413	0.145	1.322
150	0.096	0.0796	0.097	0.211
200	0.085	0.0202	0.089	0.0452
250	0.089	0.0057	0.096	0.0106
300	0.100	0.0017	0.106	0.0026

chargino case and in Figure 7 for the gaugino-like chargino case. A mass limit for stable charginos is set by observing the point of intersection between the cross section limit and the NLO cross section prediction. This results in a mass limit of 140 GeV for the higgsino-like chargino model and a mass limit of 174 GeV for the gaugino-like chargino model. These are currently the best experimental limits to date for stable charginos.

V. EFFECT OF A FINITE LIFETIME

The stau analysis and both models in the chargino analysis assumed that the CMSP's were absolutely stable. If the CMSP was to decay inside the detector it would reduce the acceptance and hence the sensitivity of this analysis. The effect of a finite lifetime CMSP was estimated by assuming the lifetime, then demanding that both of the CMSP's not decay until passing the detector's C-layer muon scintillation counters. Figure 8 shows the acceptance versus lifetime for 100 GeV staus, higgsino-like charginos, and gaugino-like charginos.

VI. CONCLUSION

A search for charged massive stable particles has been performed at the $D\bar{O}$ detector at the Fermilab Tevatron using 390 pb^{-1} of data. The timing information in the muon scintillation counters is used to calculate the speed of the muons in the event. No excess of events is observed over the background prediction, and 95% CL limits on the production cross for pair-produced stable stau leptons are set. These limits vary from 0.06 pb to 0.62 pb, depending on the stau mass, and are the most stringent limits to date from the Tevatron. Mass limits are also set for the pair-production of stable charginos. A higgsino-like chargino must be heavier than 140 GeV and a gaugino-like chargino must be heavier than 174 GeV, both at the 95% confidence level. These are currently the best limits to date on stable charginos.

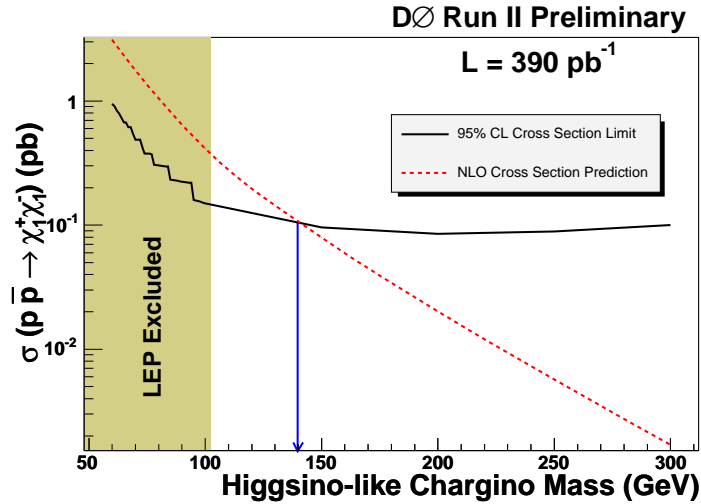


FIG. 6: 95% CL cross section for higgsino-like charginos (black) and the NLO cross section prediction (red). Stable charginos with a mass less than 140 GeV are excluded.

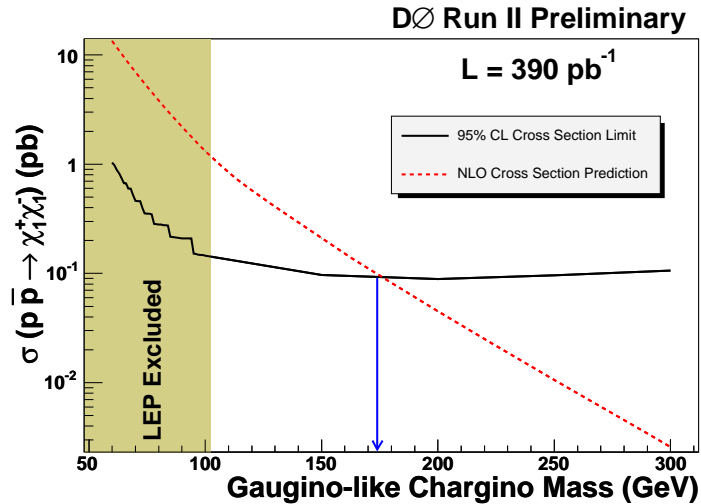


FIG. 7: 95% CL cross section for gaugino-like charginos (black) and the NLO cross section prediction (red). Stable charginos with a mass less than 174 GeV are excluded.

Acknowledgments

We thank the staffs at Fermilab and collaborating institutions, and acknowledge support from the Department of Energy, National Science Foundation, and Department of Education (USA), Commissariat à l’Energie Atomique and CNRS/Institut National de Physique Nucléaire et de Physique des Particules (France), Ministry of Education and Science, Agency for Atomic Energy and RF President Grants Program (Russia), CAPES, CNPq, FAPERJ, FAPESP and FUNDUNESP (Brazil), Departments of Atomic Energy and Science and Technology (India), Colciencias (Colombia), CONACyT (Mexico), KRF (Korea), CONICET and UBACyT (Argentina), The Foundation for Fundamental Research on Matter (The Netherlands), PPARC (United Kingdom), Ministry of Education (Czech Republic), Natural Sciences and Engineering Research Council and WestGrid Project (Canada), BMBF (Germany), A.P. Sloan Foundation, Civilian Research and Development Foundation, Research Corporation, Texas Advanced Research Program, and the Alexander von Humboldt Foundation.

We would like to acknowledge Stephen P. Martin for many fruitful discussions about the theory and production of supersymmetric particles. We also thank Michael Klasen for his assistance in calculating the NLO chargino cross

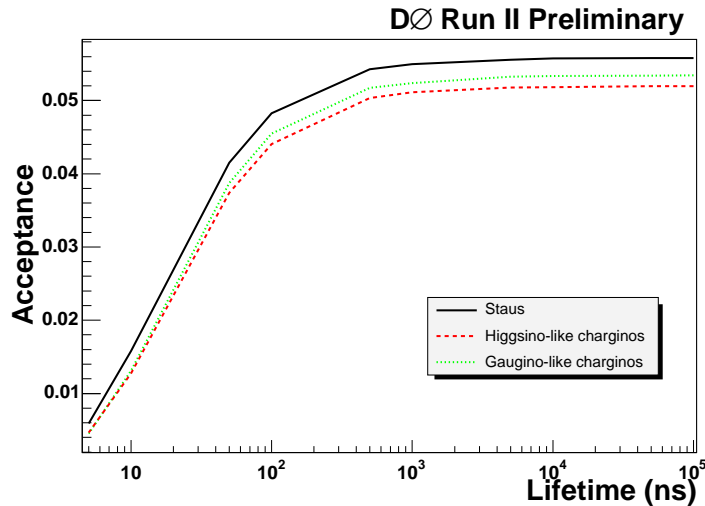


FIG. 8: Acceptance versus lifetime for staus (black), higgsino-like charginos (red), and gaugino-like charginos (green). All have a mass of 100 GeV.

sections.

-
- [1] M. Byrne, C. Kolda, and P. Regan, Phys. Rev. D **66**, 075007 (2002).
 [2] P. Smith, et. al., Nucl. Phys B **206**, 333 (1982).
 [3] M. Dine and A.E. Nelson, Phys. Rev. D **48**, 1277 (1993).
 [4] M. Dine, A.E. Nelson, Y. Nir, and Y. Shirman, Phys. Rev. D **53**, 2658 (1996).
 [5] J. Feng and T. Moroi, Phys. Rev. D **58**, 035001 (1998).
 [6] J. Feng, S. Su, and F. Takayama, Phys. Rev. D **70**, 063514 (2004).
 [7] J. Feng, S. Fu, and F. Takayama, Phys. Rev. D **70**, 075019 (2004).
 [8] S.P. Martin, S. Moretti, J. Qian, G.W. Wilson, FERMILAB-CONF-01-371-T.
 [9] J. Gunion and S. Mrenna, Phys. Rev. D **62**, 015002 (2000).
 [10] C. Chen, M. Drees, J. Gunion, Phys. Rev. D **55**, 330 (1997).
 [11] D. Acosta, et. al., Phys. Rev. Lett. **90**, 131801 (2003).
 [12] A. Heister, et. al., Eur. Phys. J. C **25**, 339 (2002).
 [13] J. Abdallah, et.al., Eur. Phys. J. C **27**, 153 (2003).
 [14] P. Achard, et.al., Phys. Lett. B **517**, 75 (2001).
 [15] G. Abbiendi, et. al., Phys. Lett. B **572**, 8 (2003).
 [16] A. Heister, et. al., Phys. Lett. B **533**, 223 (2002).
 [17] P. Abreu, et. al., Phys. Lett. B **444**, 491, 1998.
 [18] P. Abreu, et. al., Eur. Phys. J. C **11**, 1 (1999).
 [19] M. Acciarri, et. al., Phys. Lett. B **471**, 308 (1999).
 [20] G. Abbiendi, et. al., Phys. Lett. B **572**, 8 (2003).
 [21] LEP2 SUSY Working Group,
http://lepsusy.web.cern.ch/lepsusy/www/stable_summer02/stable_208.html .
 [22] T. Sjosstrand, et.al., Computer Physics Commun. **135**, 238 (2001).
 [23] T. Junk, Nucl. Instrum. Methods A **434**, 435 (1999).
 [24] B.C. Allanach, hep-ph/0104145
 [25] W. Beenakker, M. Klasen, M. Kramer, T. Plehn, M. Spira and P. M. Zerwas, Phys. Rev. Lett. **83**, 3780 (1999)
 [26] It is also possible that the right-handed smuon and selectron are nearly mass degenerate with the lightest stau, resulting in the “slepton co-NLSP” scenario.